

## Moving Wigner Glasses and Smectics: Dynamics of Disordered Wigner Crystals

C. Reichhardt,<sup>1</sup> C. J. Olson,<sup>1</sup> N. Grønbech-Jensen,<sup>2</sup> and Franco Nori<sup>3</sup>

<sup>1</sup>*Department of Physics, University of California, Davis, California 95616*

<sup>2</sup>*Department of Applied Science, University of California, Davis, California 95616*

<sup>3</sup>*Center for Theoretical Physics and Physics Department, The University of Michigan, Ann Arbor, Michigan 48109-1120*

(Received 25 July 2000)

We examine the dynamics of driven classical Wigner solids interacting with quenched disorder from charged impurities. For strong disorder, the initial motion is plastic, in the form of crossing winding channels. For increasing drive, there is a reordering into a moving Wigner smectic with the electrons moving in separate 1D channels. These different dynamic phases can be related to the conduction noise and  $I(V)$  curves. For strong disorder, we show criticality in the voltage onset just above depinning. We obtain the dynamic phase diagram for driven Wigner solids and demonstrate a finite threshold of force for transverse sliding, recently observed experimentally.

DOI: 10.1103/PhysRevLett.86.4354

PACS numbers: 73.50.-h, 73.43.Lp

Ordered arrays of charged particles have been studied in the context of colloidal suspensions, atomic-ion Wigner crystals, semiconductor heterostructures, quantum computers, astrophysics, biophysics, plasmas, and arrays of metallic islands interconnected by tunnel junctions [1]. A revival of general interest in charged arrays has been fueled by the observation, in 2D heterostructures, of nonlinear  $I$ - $V$  curves exhibiting a threshold as a function of an externally applied electric field [2,3], indicating the presence of a Wigner solid (WS) [4] that has been pinned by disorder in the sample. The depinning threshold can vary up to 2 orders of magnitude in different samples [3]. Indeed, experiments [1] based on transport and photoluminescence provide indirect evidence for the existence of the WS, and demonstrate the very important role *disorder* plays in the dynamics of the WS [5]. It is the purpose of this paper to study how disorder affects the transport properties of the driven WS.

The onset of broad-band conduction noise has been interpreted as a signature of the sliding of a defected WS [2]. If the electrons retained their order and slid collectively, narrow-band noise resembling that in sliding charge-density wave systems should appear. Simulations [6–8] on classical Wigner crystals interacting with charged defects indicate that a disorder-induced transition, from a clean to a defected WS, can occur as a function of increasing pinning strength. For strong pinning, the initial depinning is plastic and involves tearing of the electron crystal [6–8]. Many aspects of this transport have not been systematically characterized, including the current-voltage  $I(V)$  characteristics, conduction noise, transverse threshold for sliding, and the electron lattice structure for varying applied drives.

Plastic depinning has been observed in the related system of driven vortex lattices in disordered superconductors, where it is associated with flux motion through intricate riverlike channels [9,10]. Defects in the vortex lattice strongly affect the depinning thresholds and the voltage noise produced by the system. For increasing

drive the initially defected vortex lattice can *reorder* to a moving lattice or moving smectic phase [10–14]. In the fast moving lattice phase the vortex lattice regains order in both transverse and longitudinal directions with respect to the driving force, while in the smectic state only order transverse to the driving direction appears.

It is unclear *a priori* whether the same reordering transitions can occur for *long-range* pinning, such as in the WS interacting with charged impurities. This is in contrast with the vortex system, where pinning occurs only on a very short length scale. Theoretical work on the reordering transition also considered only *short-range* (and often *weak*) pinning [10–14]. In the strong pinning limit, critical behavior may occur near the depinning threshold, leading to velocity-force relations of the form  $v \sim (F - F_T)^\xi$ . As seen in transport in metallic dots,  $\xi = 5/3$  theoretically [15], and  $\xi = 2.0$  and 1.58 experimentally [16].

We use numerical simulations to study the dynamics of a 2D electron system forming a classical WS in the presence of charged impurities. For strong pinning, the electron crystal is highly defected and depins plastically, with certain electrons flowing in well-defined channels while others remain immobile. For increasing driving force, the initially disordered electrons can partially *reorder* into a moving Wigner smectic state, where the electrons flow in 1D nonintersecting channels. The reordering is accompanied by a saturation in the  $dI/dV$  curves and by a change from a broad-band to a narrow-band voltage noise signature. For weak disorder, the depinning is elastic and a narrow-band noise signal appears at all drives above depinning. For strong disorder, where the depinning is plastic, we find criticality in the velocity force curves in agreement with transport in metallic dots [15,16]. We map out the dynamic phase diagram as a function of disorder strength and applied driving force. Also, we find a finite transverse threshold for sliding conduction, in agreement with recent experiments [17]. Our results can also be tested in other systems, cited earlier in this paper.

We conduct overdamped molecular dynamics (MD) simulations using the model studied by Cha and Fertig [6,7] and Groth *et al.* [8]. The energy of the system is

$$U = \sum_{i \neq j} \frac{e^2}{|\mathbf{r}_i - \mathbf{r}_j|} - \sum_{ij} \frac{e^2}{\sqrt{(|\mathbf{r}_i - \mathbf{r}_j^{(p)}|^2 + d^2)}}. \quad (1)$$

The first term is the electron-electron (Coulomb) repulsion and the second term is the electron-impurity interaction, where the impurities are positively charged defects out of plane. Here,  $\mathbf{r}_i$  is the location of electron  $i$ , and  $\mathbf{r}_j^{(p)}$  is the in-plane location of a positive impurity located at an out-of-plane distance  $d$  (measured in units of  $a_0$ , the average lattice constant of the WS). The number (density) of electrons  $N_i$  equals the number (density) of impurities  $N_p$ , and the *disorder strength* is varied by changing  $d$ . Temperature is modeled by Langevin dynamics. The long-range Coulomb interactions are evaluated with a Lekner resummation [18]. We neglect inertial effects from damping, originating from vibrations induced by interactions with defect ions. We have also considered (here and in [8]) many other cases (e.g.,  $\pm$  charged impurities,  $N_i \neq N_p$ , etc.) with consistent results.

The initial electron positions are obtained from simulated annealing, in which we start from a high temperature state where the electrons are molten and slowly cooled to a low temperature. Once the electron configuration has been initialized, the critical depinning force is determined by applying a very slowly increasing uniform driving force  $f_d$  corresponding to an applied electric field. After each drive increment, a transient of  $10^4$  MD steps is allowed before collecting data, which we average over the next  $10^4$  time steps. For each drive increment, we measure the average electron velocity ( $\propto$  current) in the direction of drive,  $V_x = (1/N_i) \sum_i \hat{\mathbf{x}} \cdot \mathbf{v}_i$ . The  $V_x$  versus  $f_d$  curve corresponds to an  $I(V)$  experimental curve and we will thus use the notations  $V_x = I$  and  $f_d = V$ . The depinning force  $f_d^c$  is defined as the drive  $f_d$  at which  $V_x$  reaches a value of 0.01 that of the Ohmic response. We have studied system sizes  $N_i$  from 64 to 800 and find similar behavior at all sizes. Most of the results presented here are for systems with  $N_i = 256$ .

When driven through a sample containing strong pinning, the electron lattice undergoes a gradual reordering transition as the driving force is increased. We illustrate such a reordering transition in Fig. 1 by plotting the electron trajectories at increasing driving forces for a sample containing strong disorder of  $d = 0.65$ . In Fig. 1(a) the onset of motion occurs through the opening of a *single* winding channel, resembling filamentary vortex flow [9]. Electrons outside the channel remain *pinned*, and the overall system is disordered. At  $f_d/f_d^c = 1.5$ , shown in Fig. 1(b), several channels have opened, some of which are *interconnecting*. The original channel in Fig. 1(a) has grown in width, but regions of pinned electrons are still present. Electrons moving past a pinned electron perturb it, causing it to move (like a revolving door) in a circular

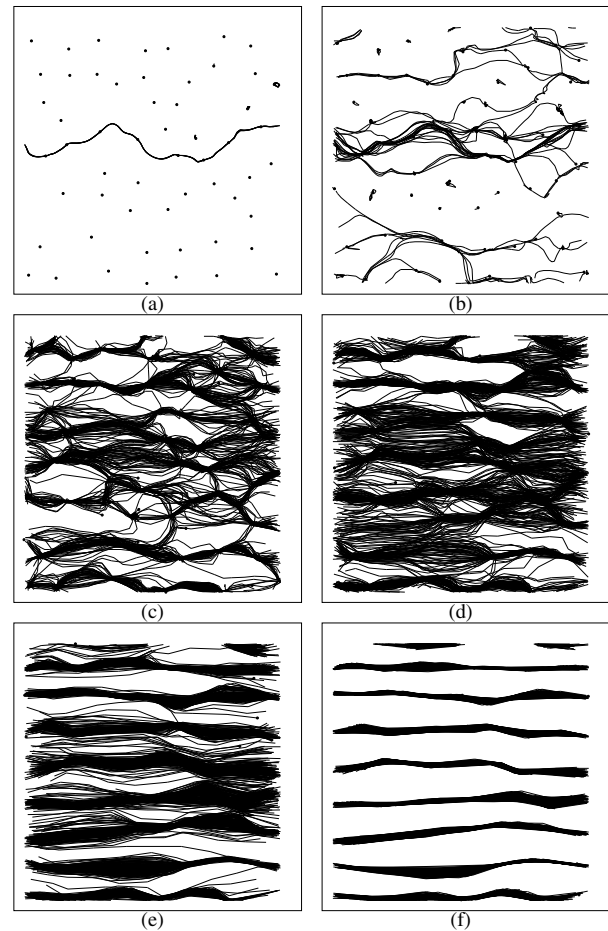


FIG 1. Electron positions (dots) and eastbound trajectories (lines) for a sample with  $N_i/N_p = 1.0$  and  $d = 0.65$ .  $f_d/f_d^c =$  (a) 1.1, (b) 1.5, (c) 2.25, (d) 3.0, (e) 4.0, and (f) 5.0.

orbit around the center of the potential minima in which it is trapped. Several of these *electron turnstiles* can be observed in Fig. 1(b). In Fig. 1(c) for  $f_d/f_d^c = 2.25$ , there are regions where electrons do not flow, but none of the electrons are permanently pinned. Some electrons become temporarily pinned before moving again. If the trajectories are drawn for a sufficiently long time, the electron flow appears everywhere in the sample, although there are still preferred paths in which more electrons flow. In Fig. 1(d) for  $f_d/f_d^c = 3.0$  the electron flow occurs more uniformly across the sample. In Fig. 1(e) at  $f_d/f_d^c = 4.0$  the electrons begin to flow predominantly in certain noncrossing channels, although some electrons jump from channel to channel. In Fig. 1(f) for  $f_d/f_d^c = 5.0$  the electron flow occurs in well-defined noncrossing channels, which can contain different numbers of electrons. A similar channel motion exists for driven vortices in disordered superconductors [10,12–14].

For samples containing very weak disorder, the pinned WS has sixfold ordering and depins elastically, without generating defects in the lattice. In this regime, the electron crystal flows in 1D channels with each channel containing the *same* number of electrons. Here, the transverse

wanderings of the electrons are considerably reduced compared to the case of strong pinning.

To better illustrate the change in the amount of disorder in the electron lattice, we show in Fig. 2(a) the Delaunay triangulation for the electrons for the same drive as in Fig. 1(f). Defects, in the form of 5–7 disclination pairs, appear with Burgers vectors oriented perpendicular to the drive direction. The computed structure factor (not shown) exhibits only two prominent peaks for order in the direction transverse to the drive, consistent with a moving Wigner smectic state. In Fig. 2(b) we show the Delaunay triangulation for the moving state in a weakly pinned sample with  $d = 1.76$ , where the initial depinning is elastic. Here the moving lattice is defect-free. The structure factor in this case shows four longitudinal peaks in addition to the two (more prominent) transverse peaks. Much larger systems would be necessary to determine whether the system is in a smectic state or in a moving Bragg glass [12] in this particular case of *weak* disorder.

To connect the reordering sequence with a measure that is readily accessible experimentally, we plot in Fig. 3(a) the  $I(V)$  and  $dI/dV$  curves. A peak occurs in  $dI/dV$  at  $f_d/f_d^c \approx 3$ , when the electrons are undergoing very disordered plastic flow. In Fig. 3(b) we plot the fraction  $P_6$  of sixfold coordinated electrons as a function of drive. A perfect triangular lattice would have  $P_6 = 1$ . For drives  $f_d/f_d^c < 2$ , the lattice is highly defected. For  $f_d/f_d^c > 3$  (i.e., past the peak in  $dI/dV$ ), the order in the lattice begins to increase. The value of  $P_6$  saturates near  $f_d/f_d^c \approx 6$  which also coincides with the saturation of the  $dI/dV$  curve. Thus the experimentally observable  $I(V)$  characteristic can be considered a good measure of the *degree* of order and the *nature* of the flow in the system. To quantify the *degree of plasticity* of the electron flow, we plot in Fig. 3(c) the fraction of electrons  $D_{tr}$  that wandered a distance of more than  $a_0/2$  in the direction *transverse* to the drive during an interval of 8000 MD steps. The peak in  $D_{tr}$  coincides with the peak in  $dI/dV$ .  $D_{tr}$  then slowly declines until it saturates at  $f_d/f_d^c \approx 6$ , indicating the *gradual* formation of the *nonintersecting channels*, as seen in

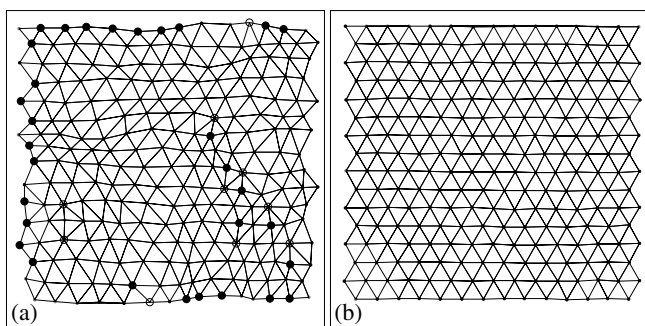


FIG 2. Delaunay triangulation for electrons in a sample with (a)  $d = 0.65$  (strong pinning) at  $f_d/f_d^c = 5.0$ , and (b)  $d = 1.76$  (weak pinning) at  $f_d/f_d^c = 2.0$ . The defects on the edges are an artifact of our triangulation algorithm. Large circles indicate (fivefold or sevenfold) defects in the electron lattice.

Fig. 1(f). The saturation in  $D_{tr}$  coincides with the saturations in both  $P_6$  and  $dI/dV$ . It is beyond the scope of this paper to determine whether the reordering transition is a true phase transition; however, we do not observe any hysteresis in the measured quantities through the reordering sequence.

The  $I(V)$  curve in Fig. 3(a) corresponds to a highly irregular voltage signal as a function of time when the electrons are in the plastic flow regime ( $f_d/f_d^c = 1.5$ ). The corresponding voltage noise spectrum in the inset of Fig. 3(c) shows that only broad-band noise is present. In contrast, at  $f_d/f_d^c = 4.0$ , in the moving smectic regime, a roughly regular signal is obtained, and narrow-band noise appears, as shown in the inset of Fig. 3(c). In a system with  $d = 1.57$  when the depinning is elastic only, an even more pronounced narrow-band noise signal is observable. In experiments, broad-band noise was observed above depinning [2], but narrow-band noise has not been seen. Our results suggest that *plasticity* may be playing an important role in most experiments.

In Figs. 3(d) and 3(e), we examine the critical behavior above the depinning threshold of  $V_x$  versus  $f_d$  for disorder strengths  $d = 0.5$  and  $0.65$ . In Fig. 3(d),  $V_x \sim [(f_d - f_d^c)/f_d^c]^\xi$ , so that the curves are fit well by a power law with  $\xi = 1.61 \pm 0.10$  and  $1.71 \pm 0.10$ . These values agree well with the predicted value of  $\xi = 5/3$  [15] for

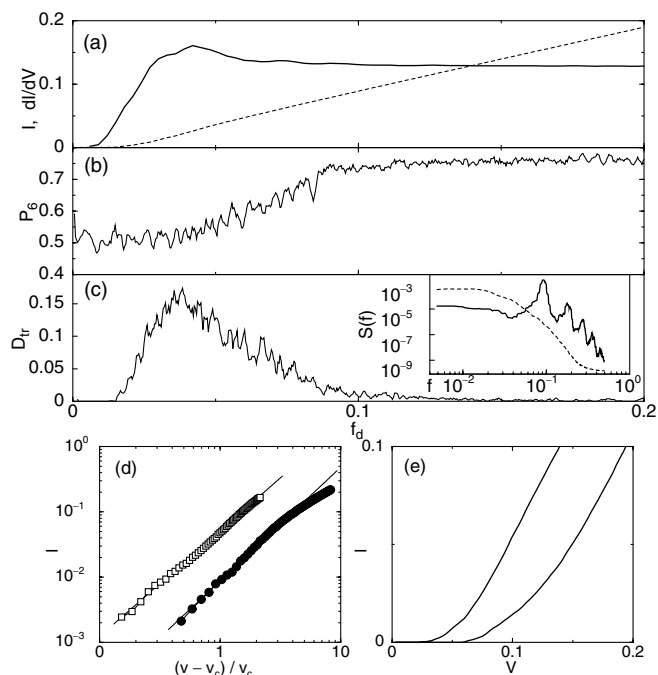


FIG 3. (a)  $I(V)$  (dashed line) and  $dI/dV$  curves (solid line) for a sample with  $d = 0.65$ . (b) Fraction  $P_6$  of sixfold coordinated electrons, as a function of driving force  $f_d$ . (c) Fraction  $D_{tr}$  of transversely wandering electrons. Inset to (c): noise spectra for  $f_d/f_d^c = 1.5$  in the plastic flow regime showing broad-band noise (dashed line) and for  $f_d/f_d^c = 4.0$  in the smectic regime showing a narrow-band signal (solid line). (d)  $V_x = (f_d - f_d^c)^\xi$ , in which  $\xi = 1.61 \pm 0.10$  and  $1.71$ . (e)  $V_x$  versus  $f_d$  for disorder strengths of  $d = 0.5$  and  $0.65$ .

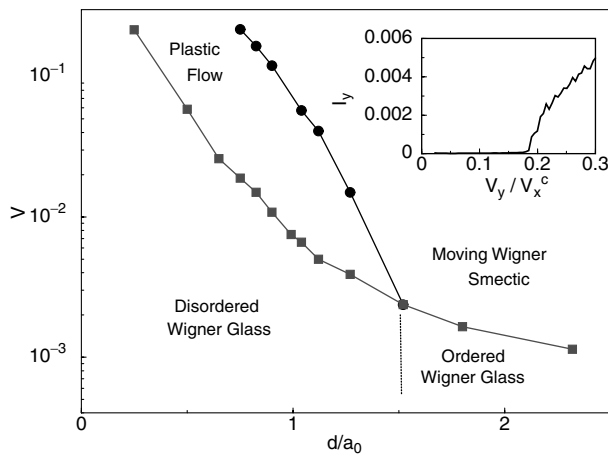


FIG 4. Dynamic phase diagram for the driven disordered Wigner solid. Inset: clear evidence for a finite transverse depinning threshold for a system with  $d = 0.9$  at  $f_d = 0.16$  in the reordered phase.

electron flow through disordered arrays, and the experimentally observed values of  $\xi = 1.58$  and  $2.0$  [16]. A proposal [12] on the moving ordered phase (for very weak and very short-range pinning) predicts a barrier to transverse motion once channels similar to those in Fig. 1(e) form. As shown in the inset of Fig. 4, for a system in the reordered phase we observe a transverse depinning threshold that is about  $1/6$  the size of the longitudinal depinning threshold  $f_d^c$ . In recent experiments, Perruchot *et al.* [17] also found evidence for a transverse barrier that is about  $1/10$  the size of the longitudinal threshold. These thresholds are much larger than those observed in vortex matter interacting with short-ranged pinning, where ratios of  $1/100$  are seen [14].

In Fig. 4 we present the *dynamic phase diagram* as a function of disorder strength and driving force. For  $f_d = 0$  we observe a similar static ordering as in [6,7] where, for strong disorder ( $d < 1.4$ ), the electron lattice is considerably defected, the structure factor is a liquid-like ring, and the depinning is plastic. We label this static region the disordered Wigner glass which depins into the plastic flow regime. For weak disorder there are few or no defects and the depinning transition is elastic. We label this region the ordered Wigner glass. For decreasing  $d$ , the pinned region grows while a reordering transition to a *moving Wigner smectic* state occurs for higher drive. For  $f_d = 0$  a hexatic phase may exist; however, much larger simulations would be required to resolve this issue.

In summary, we have investigated the dynamics of an electron solid interacting with charged disorder. We find that for strong disorder the depinning transition is plastic with electrons flowing in a network of winding channels. For increasing drives, the electrons partially reorder and flow in nonintersecting channels forming a moving Wigner smectic. We show that the onset of these different phases can be inferred from the transport characteristics. In the plastic flow regime, the noise has broad-band characteris-

tics, while, in the moving smectic or elastic flow phase, a narrow-band noise signal is observable. We also find critical behavior at the onset of the plastic flow phase, with critical exponents in agreement with predictions for transport in arrays of metallic dots [15,16]. We map out the dynamic phase diagram as a function of disorder and applied driving force. We obtain a finite threshold for transverse sliding, in agreement with recent experiments [17].

We acknowledge J. Groth and A.M. MacDonald for very useful discussions, and B. Janko for his kind hospitality. This work was partially supported by DOE Office of Science No. W-31-109-ENG-38, CLC and CULAR (LANL/UC), NSF DMR-9985978. F.N. also acknowledges partial support from CSCS and MCTP at the UM.

- [1] See, e.g., *2D Electron Systems on Helium and Other Substrates*, edited by E. Y. Andrei (Kluwer, New York, 1997), and references therein.
- [2] See, e.g., V.J. Goldman *et al.*, Phys. Rev. Lett. **65**, 2189 (1990); Y.P. Li *et al.*, Phys. Rev. Lett. **67**, 1630 (1991).
- [3] See, e.g., F.I.B. Williams *et al.*, Phys. Rev. Lett. **66**, 3285 (1991); H.-W. Jiang *et al.*, *ibid.* **44**, 8107 (1991).
- [4] See, e.g., A.H. MacDonald and S.M. Girvin, Phys. Rev. B **38**, 6295 (1988); R. Cote and A.H. MacDonald, *ibid.* **44**, 8759 (1991); B.G.A. Normand, P.B. Littlewood, and A.J. Millis, *ibid.* **46**, 3920 (1992); R. Cote and A.H. MacDonald, Phys. Rev. Lett. **65**, 2662 (1990); M.I. Dykman and Y.G. Rubo, *ibid.* **78**, 4813 (1997); E. Fradkin *et al.*, *ibid.* **84**, 1982 (2000).
- [5] See, e.g., D. Shahar *et al.*, Phys. Rev. Lett. **74**, 4511 (1995); S.T. Chui and B. Tanatar, *ibid.* **74**, 458 (1995).
- [6] M.-C. Cha and H.A. Fertig, Phys. Rev. Lett. **73**, 870 (1994).
- [7] M.-C. Cha and H.A. Fertig, Phys. Rev. B **50**, 14369 (1994).
- [8] J. Groth, O. Pla, A.H. MacDonald, and F. Nori, Bull. Am. Phys. Soc. **39**, 207 (1994).
- [9] See, e.g., F. Nori, Science **271**, 1373 (1996); H.J. Jensen *et al.*, Phys. Rev. Lett. **60**, 1676 (1988); N. Grønbech-Jensen *et al.*, *ibid.* **76**, 2985 (1996); C.J. Olson *et al.*, *ibid.* **80**, 2917 (1998).
- [10] C.J. Olson, C. Reichhardt, and F. Nori, Phys. Rev. Lett. **81**, 3757 (1998).
- [11] A.E. Koshelev and V.M. Vinokur, Phys. Rev. Lett. **73**, 3580 (1994).
- [12] T. Giamarchi and P. Le Doussal, Phys. Rev. Lett. **76**, 3408 (1996); **78**, 752 (1997).
- [13] L. Balents *et al.*, Phys. Rev. B **57**, 7705 (1998).
- [14] K. Moon, R.T. Scalettar, and G.T. Zimányi, Phys. Rev. Lett. **77**, 2778 (1996); S. Ryu *et al.*, *ibid.* **77**, 5114 (1996); S. Spencer and H.J. Jensen, Phys. Rev. B **55**, 8473 (1997); C.J. Olson and C. Reichhardt *ibid.* **61**, R3811 (2000).
- [15] A.A. Middleton and N.S. Wingreen, Phys. Rev. Lett. **71**, 3198 (1993).
- [16] C. Kurdak *et al.*, Phys. Rev. B **57**, R6842 (1998).
- [17] F. Perruchot *et al.*, Physica (Amsterdam) **284B-288B**, 1984 (2000).
- [18] N. Grønbech-Jensen *et al.*, Mol. Phys. **92**, 941 (1997).